doi: 10.4149/gpb_2022039

Homocysteine promotes migration of adventitial fibroblasts *via* angiotensin II type 1 receptor activation to aggravate atherosclerosis

Zhibo Zhu[1,2], Sujuan Li[3], Yuchen Jia[4] and Jianqiang Guo[1]

[1] *Department of Cardiology, The Affiliated Hospital of Inner Mongolia Medical University, Inner Mongolia, China*
[2] *Nuclear Medicine Department, Chifeng Municipal Hospital, Chifeng, Inner Mongolia, China*
[3] *Department of Gastroenterology, The Affiliated Hospital of Inner Mongolia Medical University, Inner Mongolia, China*
[4] *Inner Mongolia Key Lab of Molecular Biology, School of Basic Medical Sciences, Inner Mongolia Medical University, Inner Mongolia, China*

Abstract. This study clarified the effect of homocysteine on adventitial fibroblasts (AFs) and its relationship with angiotensin II type 1 receptor (AT1R). Hyperhomocysteinemia aggravated the plaque area and increased the expression of IL-6, MCP-1, and macrophage infiltration in the plaque and adventitia of the aorta, whereas telmisartan improved this effect. Hyperhomocysteinemia induced the occurrence of the AFs marker protein ER-TR7 in the plaque and entire layer of the aorta, whereas telmisartan improved these effects, indicating that homocysteine induced AFs migration and that AT1R mediated this process. The migration experiments of AFs also reached the same conclusion. Homocysteine increased the phosphorylation levels of PKC and ERK1/2 in the AFs and HEK293A cells transfected with the AT1R plasmid, whereas telmisartan inhibited this effect, indicating that homocysteine activated AT1R intracellular signaling pathway. Homocysteine also increased the AFs At1R expression. Conclusion, homocysteine promoted adventitial inflammation, induced AFs migration, and aggravated atherosclerosis by activating AT1R.

Key words: Homocysteine — Angiotensin II type 1 receptor — Adventitial fibroblasts — Migration — Atherosclerosis

Introduction

Hyperhomocysteinemia (HHcy) (circulating homocysteine ≥ 15 μm) is an independent risk factor for many cardiovascular diseases, such as atherosclerosis, coronary heart disease, and abdominal aortic aneurysm. Although there is evidence that HHcy can damage endothelial cells, promote intravascular proliferation, promote outer membrane activation, and disrupt hemostasis/coagulation (Liu et al. 2012; Zhang et al. 2012; Sun et al. 2015; Duan et al. 2016; Li et al. 2018), the mechanism by which homocysteine (Hcy) aggravates atherosclerosis remains elusive.

AT1R is a key player in the renin-angiotensin system. AT1R activation leads to cardiac remodeling, ventricular hypertrophy, intimal formation, smooth muscle cell proliferation, and migration (Kassab et al. 2006; Zhao YS et al. 2019). Although recent studies indicate homocysteine directly interacts and activates AT1R to aggravate vascular injury in abdominal aortic aneurysm (AAA) mouse model (Li et al. 2018) and homocysteine accelerates collagen accumulation in the adventitia of balloon-injured rat carotid arteries *via* AT1R expression (Yao et al. 2014), little is known about the association between homocysteine and AT1R in adventitial fibroblasts.

Migration and proliferation responses of cells in the vascular wall and deposition of extracellular matrix (ECM) play

Correspondence to: Jianqiang Guo, Department of Cardiology, The Affiliated Hospital of Inner Mongolia Medical University, Inner Mongolia, China
E-mail: gjq161208@126.com

a key role in restenosis and atherosclerosis (Siow et al. 2003). Although medial smooth muscle cells have been regarded as the main source of cells (Zou et al. 2010; Xu et al. 2019), there is now increasing evidence that the adventitial layer can also be a significant contributor to the arterial remodelling process through increased angiogenesis (Xu et al. 2015). Siow et al. (2003) provided direct evidence that adventitial fibroblasts migration contribute to neointima formation after balloon injury. However, the precise role of homocysteine in the migration and invasion of adventitia fibroblasts is unclear in the process of atherosclerosis formation.

Therefore, we investigated whether HHcy stimulates AFs migration and invasion in mice *via* AT1R activation to accelerate the formation atherosclerosis.

Materials and Methods

Materials

L-homocysteine (69453), telmisartan (T8949), was purchased from Sigma-Aldrich. Disposable consumables such as cell culture bottle and 6-well plates were purchased from Guangzhou Jet Bio-Filtration Co., Ltd.

Animals and treatments

A total of 21 ApoE$^{-/-}$ mice (male, 8 weeks) were purchased from Beijing Vital River Laboratory Animal Technology Co., Beijing, China (Ltd. Number: SCXK2016-0006). The mice were randomly divided into three groups: a Control group with a standard mouse diet ($n = 7$), an HHcy group fed with standard mouse diet plus 1.5% methionine ($n = 7$) (Yang et al. 2015; Yang et al. 2020), and a telmisartan gavage group (HHcy+Telmi) treated with telmisartan (10 mg/kg/day) (Fukuda et al. 2010). Ten Sprague Dawley rats (male, weighing 150–200 g) were purchased from Inner Mongolia Medical University Laboratory (Hohhot, China). All animal experiments were conducted in accordance with the Guide for the Care and Use of laboratory animals from the National Institutes of Health (Bethesda, MD, USA).

Tail-cuff measurement of systolic blood pressure

Systolic blood pressure (SBP) was recorded by a computerized non-invasive tail-cuff system (Cat. NO. BP-300A, Chengdu Techman Software CO., LTD). Measurements were performed in quiet environment to avoid causing mice anxiety. The mice underwent 7 consecutive days of training sessions to become accustomed to the tail-cuff procedure. Blood pressure of mice underwent 12 consecutive weeks was measured from 1 to 6 p.m. on weekends every week. Three measurements were weekly performed on each mouse, so that the average of total of 3 measurements was represented as the SBP of each mouse (Li et al. 2018).

Measurement of serum homocysteine level

The levels of triglyceride (TG), total cholesterol (TC), high-density lipoprotein (HDL), and low-density lipoprotein (LDL) were assessed with kits from Beijing Sino-UK Institute of Biological Technology. homocysteine concentration was measured using enzyme-linked immunosorbent assay (HY-N0080) in Beijing Sino-UK Institute of Biological Technology.

Histology and immunostaining

The heart and approximately 2 mm of proximal aortas were fresh frozen in optimal cutting temperature (OCT) compound. Tissue samples were cut into 7-μm thin slices. Frozen tissue sections were stained with Oil Red O, H&E, Masson, and immunostaining (Venegas-Pino et al. 2013; Vendrov et al. 2017). A Masson's trichrome staining kit was used to detect collagen deposition in the atherosclerotic plaque and analyzed with Image-ProPlus 6.0 or ImageJ software (Vendrov et al. 2017). Cryosections were fixed in 4% paraformaldehyde and subsequently treated with H_2O_2 and after the primary antibody was blocked in 5% goat serum (1:100) at 4°C overnight. The tissue sections were washed in phosphate-buffered saline (PBS) then incubated with secondary antibody (1:100). They were incubated in diaminobenzidine until a change in color was observed under the microscope and then the nucleus was stained with hematoxylin (He et al. 2019). Immunofluorescence staining procedure was similar to immunostaining.

Primary rat AFs

Cells were prepared according to common methods (Xu et al. 2017) and with some modifications. The thoracic aortas of Sprague Dawley rats were removed and cleaned under sterile conditions. The adventitia was stripped from the aorta and cut into pieces about 2–3 mm^3 in size according to the method of Yong-Gang Zhang et al. (Zhang et al. 2008). Briefly, place the isolated aorta in a Petri dish with sterile PBS and rinse the blood around the vessel. Then cut the blood vessel longitudinally with ophthalmic scissors, spread the intima side of the blood vessel on the Petri dish, fix the blood vessel with one curved ophthalmic forceps, and gently scrape the intima with the back of the other curved forceps; then fix one end of the blood vessel and use Ophthalmic curved forceps strip the media longitudinally, and the remaining translucent tissue is mainly the adventitia of blood vessels. Then, the tissue pieces were attached to the 6-well plates and immersed in Dulbecco's modified Eagle's medium (DMEM, Gibco) containing 30% fetal bovine serum (FBS, Gibco) and maintained at 37°C, 5% CO_2. Cells were collected, and when

the cells grew to about 70–80% fusion, the tissue pieces could be cultured again. AFs were verified by positive immunofluorescent staining of vimentin and ER-TR7. The AFs after passage were cultured in DMEM supplemented with 10% FBS at 37°C, 5% CO_2. All AFs used in this study were from early passage with a maximum of four passages.

The human embryonic kidney cell line HEK293A was a generous gift from our laboratory and cultured in DMEM (high glucose) supplemented with 10% FBS at 37°C in a humidified atmosphere containing 5% CO_2. The cells were confirmed of no mycoplasma contamination before application.

Cell proliferation assay

The proliferation of cells was examined with Cell Counting Kit-8 (Cat. No. K1018, ApexBio Technology LLC). Briefly, cells were seeded in 96-well plates with 5×10^3 cells/well, cultured for 24 h, and subjected to the indicated treatment (Lu et al. 2019). The absorbance at 450 nm was measured using an automatic microplate reader ($n = 3$).

Wound-healing assay

AFs (5×10^5 cells/well) were inoculated into 6-well plates. After the cells completely covered the bottom wall of the 6-well plate, three vertical lines were drawn in the 6-well plate with a sterile 200 μl pipette tip, and the floating cells were removed by PBS washing (Wang et al. 2015). DMEM 1000 μl containing 1% FBS and homocysteine 200 μmol/l was added into the 6-well plate. The cells were cultured in an incubator at 37°C and 5% CO_2 for 48 h. At the same location, the images of 0 and 48 h were taken to observe the cell migration. Cell migration analysis was processed by Image-ProPlus 6.0 software (Wang et al. 2015) ($n = 3$).

Transwell matrigel invasion assays

Transwell matrigel invasion assays were performed using a transwell membrane (8 μm pore size, 6.5-mm diameter; Cat. No. 35488, Corning Incorporated) in a 24-well plate. The homocysteine-treated cells were digested with trypsin (0.25%) and then centrifuged and the supernatant was discarded. The cell suspension was prepared with DMEM without serum. The cells (1×10^5 cells/well) were loaded to the upper side of the chamber (500 μl/well), and the lower chambers contained 750 μl/well of DMEM with 10% FBS as chemoattractant. The cells were cultured in the cell incubator for 6 h. The filter inserts were then removed from the wells. Cells on the upper surface of the filter were removed using cotton swabs and the membranes were fixed and stained with crystal violet reagent (Snigireva et al. 2019). Invasion was quantified by counting 5 random fields under a light microscope (Leica, Germany) at ×40 magnification.

Detection of intracellular reactive oxygen species (ROS)

Intracellular ROS generation was monitored by using Reactive Oxygen Species Assay Kit (WLA070a, Wanleibio). Cells (1×10^6 cells/well) were seeded in 6-well plates. Cells were treated with homocysteine for 48 h and stained with 20 μmol/l DCF-DA in culture medium for 30 min in the dark. The cells were then harvested and washed in PBS three times and oxidation-induced DCF fluorescence was assayed by fluorescence microscopy (Zhao et al. 2019).

Assay of hydrogen peroxide level

Hydrogen peroxide level was assayed using a Hydrogen Peroxide Assay Kit (Cat. No. A064-1-1, Nanjing Jiancheng Bioengineering Institute, China) according to the manufacturer's instructions.

Western blot analysis

Protein extracts (40 μg) were resolved by 10% SDS-PAGE for Western blot analysis. The blots were subsequently incubated with primary antibodies (AT1R, 1:300, Abcam, ab124734; p-PKC, 1:1000, Cell Signaling Technology, 9371s; t-PKC, 1:1000, Wanleibio, WL02234; p-ERK1/2, 1:1000, Cell Signaling Technology, 9101s; t-ERK1/2, 1:1000, Cell Signaling Technology, 9102s). The corresponding secondary antibody was added for incubation at room temperature. The protein expressions in different samples were detected using the enhanced chemiluminescence method.

Statistical analysis

All data were expressed as mean ± standard error of the mean (SEM), except Table 1 and Table 2 (mean ± standard deviation). All experiments were repeated at least three times. The data were analyzed by GraphPad Prism 5.0 (GraphPad Software, San Diego, California, USA) and SPSS version 19.0 (SPSS Inc., Chicago, IL, USA). The data were analyzed by one-way ANOVA or repeated measurement ANOVA, without assuming sphericity. When multiple measurements were made in the same cell, Greenhouse-Geisser correction was performed. The data that failed to pass the normality test were analyzed by nonparametric test. The difference was significant ($p < 0.05$).

Results

Vital parameters

HHcy was induced by feeding $ApoE^{-/-}$ mice a high-methionine diet for 12 weeks. The results showed that serum homo-

Table 1. Effect of telmisartan on homocysteine and lipid levels

Parameter (μmol/l)	Group			F	*p*
	Control	HHcy	HHcy+Telmi		
Hcy	23.85 ± 2.09	35.89 ± 3.26*	17.32 ± 3.94#	3.54	0.05
TG	1.07 ± 0.53	1.21 ± 0.36	0.88 ± 0.28	1.40	0.27
TC	10.26 ± 1.47	12.72 ± 0.55*	8.76 ± 1.59#	5.42	0.01
LDL	3.03 ± 0.57	3.61 ± 0.72	2.68 ± 0.31#	3.50	0.05
HDL	1.64 ± 0.27	1.27 ± 0.21*	1.95 ± 0.11#	4.91	0.02

Homocysteine and lipid levels were measured in five to seven mice *per* group (5 mice in the Control group and 7 mice in the other groups). Data represent mean ± SEM. * $p < 0.05$ *vs.* Control group. # $p < 0.05$ *vs.* HHcy group. Control, standard mouse diet group; HHcy, standard mouse diet plus 1.5% methionine group; HHcy+Telmi, HHcy + telmisartan (10 mg/kg/day) treatment group. HHcy, hyperhomocysteinemia; Hcy, homocysteine; TG, triglyceride; TC, total cholesterol; LDL, low-density lipoprotein; HDL, high-density lipoprotein.

Table 2. Comparison of body weight before and after treatment

	Group			F	*p*
	Control	HHcy	HHcy+Telmi		
Weight before (g)	22.74 ± 1.46	22.79 ± 0.92	23.19 ± 0.81	2.22	0.32
Weight after (g)	26.73 ± 0.91	28.66 ± 1.29	25.89 ± 1.29	2.14	0.14

Weight was measured in five to seven mice per group (5 mice in the control group and 7 mice in the other groups). Data represent mean ± SD. Weight before, the weight of mice without 1.5% methionine diet and telmisartan gavage; Weight after, the weight of mice underwent 12 consecutive weeks after receiving 1.5% methionine diet and telmisartan gavage. For abbreviations, see Table 1.

cysteine concentrations in the HHcy group were significantly higher (35.89 ± 3.26 μmol/l) than the Control group (23.85 ± 2.09 μmol/l), ($p < 0.05$). Therefore, the high-methionine diet significantly increased serum concentrations of homocysteine, suggesting that the diet-induced HHcy model was successful (Table 1). TC and HDL in HHcy group were significantly different except TG. TC level in HHcy group was higher than that in Control group ($p < 0.05$). TC decreased significantly after telmisartan treatment ($p < 0.05$). LDL level in HHcy group was higher than that in Control group, but there was no statistical significance. After telmisartan treatment, LDL decreased significantly ($p < 0.05$), as shown in Table 1.

Telmisartan treatment decreased systolic blood pressure. In HHcy+Telmi group, the systolic blood pressure of mice after treatment was lower than that before treatment ($p < 0.01$); however, there was no statistical difference in three groups, showing no significant changes in body weight (Tables 2 and 3).

Table 3. Comparison of **s**ystolic blood pressure (SBP) before and after treatment

	Group		
	Control	HHcy	HHcy+Telmi
SBP before (mmHg)	119 ± 4.97	125 ± 10.29	121 ± 9.01
SBP after (mmHg)	120 ± 4.41	121 ± 6.08	113 ± 7.05
p	0.23	0.15	0.00

SBP was measured in five to seven mice *per* group (5 mice in the control group and 7 mice in the other groups). SBP before: the SBP of mice without 1.5% methionine diet and telmisartan gavage. SBP after: the SBP of mice underwent 12 consecutive weeks after receiving 1.5% methionine diet and telmisartan gavage. For abbreviations, see Table 1.

HHcy accelerates atherosclerosis formation and aggravates plaque inflammation

A large amount of lipid deposition was found in the aortic root of mice in the HHcy group. Oil red O staining showed that the atherosclerotic plaque area in the HHcy group accounted for about 23.1% of the cross-sectional area of the aortic root, compared with 6.3% in the Control group and 9.1% in the HHcy+Telmi group (Fig. 1A).

Hematoxylin and eosin staining showed higher number of foam cells and a larger acellular necrotic core area in the HHcy group, which was improved in the HHcy+Telmi group (Fig. 1B). Moreover, Masson staining (Fig. 1C) showed that total collagen content, expressed as a percentage of the sec-

tion area, was significantly reduced in HHcy group compared with that in Control group ($p < 0.001$), while it was significantly increased in the HHcy+Telmi group.

Moreover, the number of inflammatory cytokines such as MCP-1, IL-6, and Mac3 in aortic root plaques in HHcy group was significantly higher than that in Control group ($p < 0.05$) while it was reduced in the HHcy+Telmi group (Fig. 2).

HHcy amplifies aortic adventitial inflammation in ApoE$^{-/-}$ male mice

Results showed that inflammatory cells MCP-1, IL-6, and Mac3 were preferentially produced in the adventitial layer. Quantitative analysis of aortic adventitia revealed higher expression of MCP1, IL-6, and Mac3 in the HHcy group than in Control group. Furthermore, the AT1R blocker telmisartan markedly attenuated MCP1, IL-6, and Mac3 expression (Fig. 3A, B), which is consistent with observations in a previous study (Liu et al. 2012).

HHcy induces AFs migration in ApoE$^{-/-}$ male mice

Immunofluorescence was used to detect AFs marker ER-TR7. In the Control group, staining showed ER-TR7 expression in aortic adventitia. Moreover, deposition of ER-TR7 increased in the whole aortic wall and plaque in the HHcy group. This phenomenon was reduced by telmisartan, as shown in the HHcy+Telmi group (Fig. 3C).

Hcy upregulates proinflammatory effects and expression of MMP-9 in AFs

Our results showed that homocysteine of 200 μmol/l greatly enhanced hydrogen peroxide (H_2O_2) secretion (Fig. 4A)

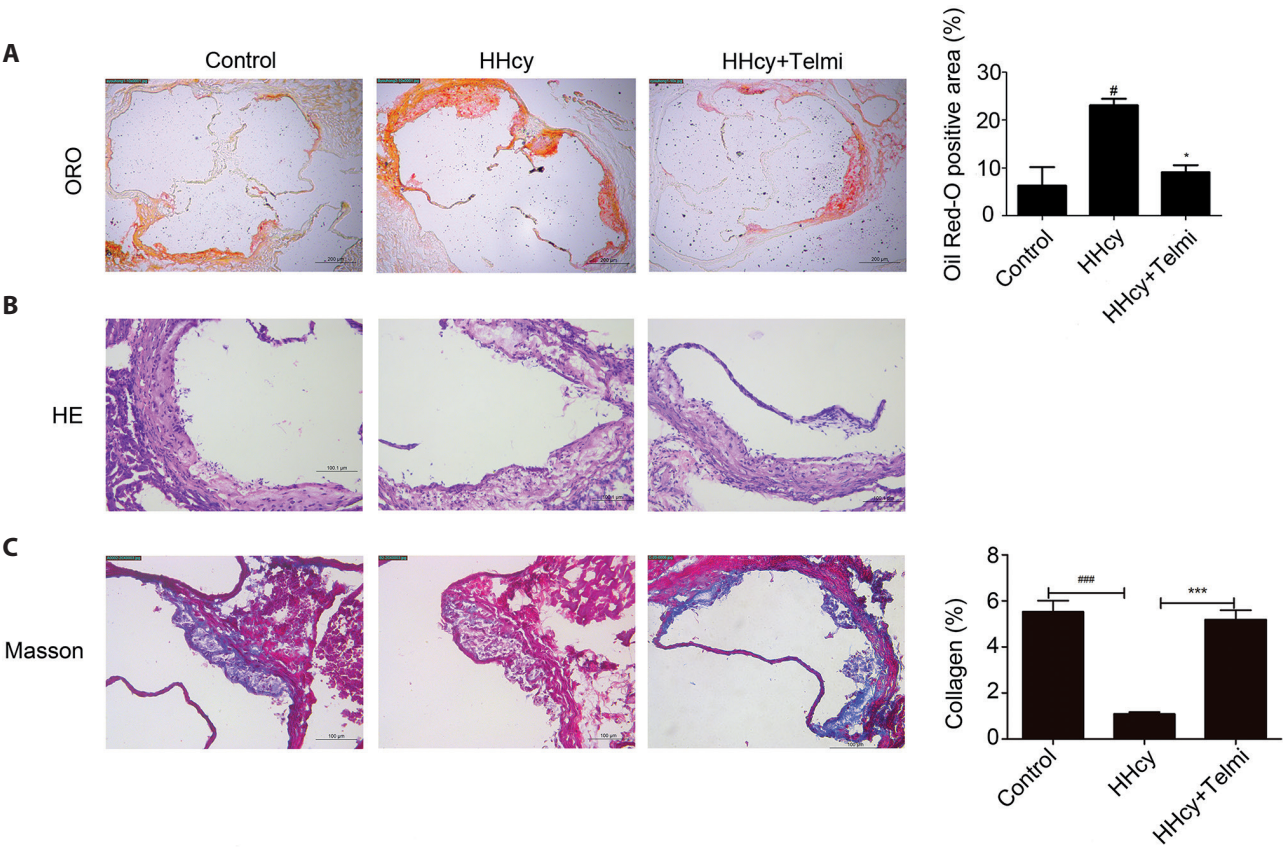

Figure 1. HHcy accelerates atherosclerosis formation and increases features of plaque instability. **A.** Representative Oil Red O (ORO) staining of the thoracic aorta root sections. The plaque area was presented as lesion% (% of whole aorta) ($n = 6$ sections *per* mice). Magnification: ×100. Scale bars = 200 μm. $^{\#}$ $p < 0.05$ *vs.* Control; * $p < 0.05$ *vs.* HHcy. **B.** Representative H&E staining. Magnification: ×200. Scale bars = 100 μm. **C.** Representative Masson staining. Collagen fibers showed as blue. Magnification: ×200. Scale bars = 100 μm. The percent of the positively stained area to the measured visual field area was reported, collagen content analysis was carried out using ImageJ software. $^{\#\#\#}$ $p < 0.001$ *vs.* Control; *** $p < 0.001$ *vs.* HHcy. Values represent mean ± SEM, $n = 3$ mice for each group. Data were analyzed by one-way ANOVA. Control, standard mouse diet group; HHcy, standard mouse diet plus 1.5% methionine group; HHcy+Telmi, HHcy + telmisartan (10 mg/kg/day) treatment group. (See online version for color figure.)

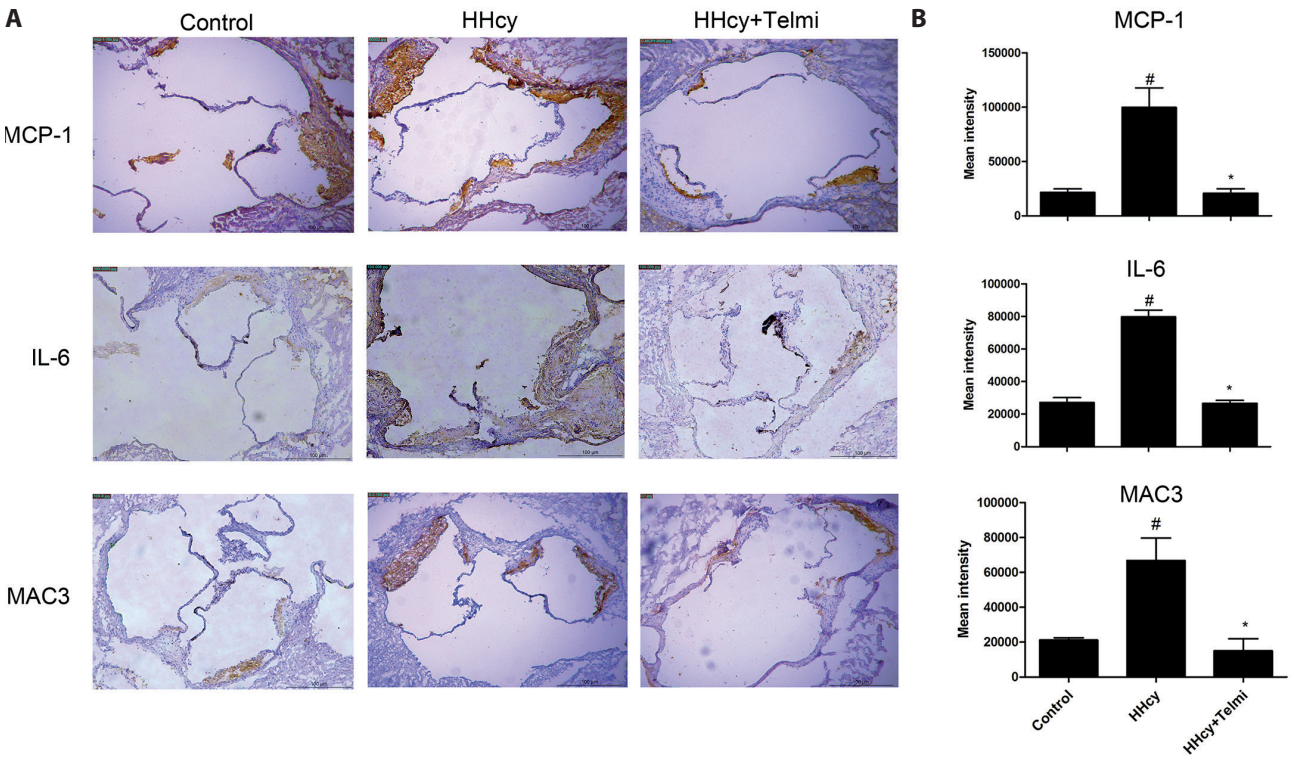

Figure 2. HHcy promoted inflammation of plaques in ApoE$^{-/-}$ male mice. **A.** Immunohistochemical staining shows MCP-1, IL-6, and Mac3 expression in each group. Magnification: ×100. Scale bar = 100 μm. **B.** Quantitative analysis of MCP-1, IL-6, and Mac-3 infiltration in atherosclerotic plaques of aortic roots (n = 3 mice for each group). Data represents mean ± SEM. The data were analyzed by one-way ANOVA. $^{\#}$ $p < 0.05$ *vs.* Control; * $p < 0.05$ *vs.* HHcy. MCP-1, monocyte chemoattractant protein-1; IL-6, interleukin-6; Mac3, macrophages. For more abbreviations, see Figure 1.

and increased intracellular ROS at 48 h after stimulation (Fig 4B). homocysteine induced IL-6 and MMP-9 expression in a time-dependent manner, and the most effective homocysteine time was 36 h as indicated by using Western blot (Fig. 4C, D). These results demonstrated that homocysteine could activate AFs oxidative stress and inflammatory response. Matrix remodeling is a critical step to initiate and support AFs motility.

Hcy induces AFs proliferation, migration and invasion of AFs

AFs were treated with increasing concentrations of homocysteine (0, 50, 100, 200, and 400 μmol/l) for 48 h. Results showed that cell viability was increased significantly in a dose-dependent manner, indicating that homocysteine promoted cell proliferation (Fig. 5A). Cells were treated with 200 μmol/l homocysteine for 48 h. The wound areas of the cells were observed *via* scratch assay under a microscope at 0 h and 48 h. Results showed that homocysteine significantly increased cell migration (Fig. 5B). Cell invasion was detected by transwell Matrigel invasion assays. In AFs stimulated by 200 μmol/l homocysteine for 48 h, cell invasion was significantly increased (Fig. 5C). After telmisartan (10 μmol/l) pretreatment for 1 h, this phenomenon was inhibited.

Hcy enhances AT1R expression in cultured AFs

Hcy induced AT1R expression in a time-dependent manner and a concentration-dependent manner as indicated by using Western blot (Fig. 6A, B). There was a significant increase in AT1R expression at 36 h (Fig. 6A). Moreover, homocysteine of 50 to 300 μmol/l significantly facilitated AT1R expression, with a peak at 200 μmol/l (Fig. 6B). This phenomenon was further verified by immunofluorescence staining of AT1R protein (Fig. 6C). We also noticed that the expression level of AT1R showed a slight decrease after 48 h of homocysteine stimulation and when the concentration above 300 μmol/l was used, which may be regulated by negative feedback. The exact reason for this phenomenon needs to be further explored.

Hcy activates AT1R signaling

We assessed G protein-dependent signaling PKC and ERK1/2 phosphorylation in AFs. The phosphorylation of ERK1/2 and PKC was increased after stimulated with homocysteine (200 μmol/l), which was decreased by telmisartan pretreatment (10 μmol/l) (Fig. 6D). To further verify the results, we constructed AT1R expression plasmid and transfected HEK293A cells to assess the effect of homocysteine on PKC and ERK1/2 signaling pathways. Western blot indicated higher AT1R expression in plasmids transfected into HEK293A cells than in the Control group (Fig. 7A), indicating that the plasmid was successfully constructed and transfected into HEK293A cells. In HEK293A cells transfected with AT1R, homocysteine at 200 μmol/l resulted in delayed but sustained PKC and ERK1/2 phosphorylation, which was decreased by telmisartan pretreatment (10 μmol/l) (Fig. 7B). These results suggested that homocysteine could activate the downstream PKC and ERK1/2 signaling pathway downstream of AT1R.

Discussion

It is well known that homocysteine can cause vascular injury, atherosclerosis, and AFs are involved in this process. Siow et al. (2003) proved that AFs can migrate from the outer membrane to the neointima after balloon injury in rats. The outer membrane plays a pathogenic role by producing large amounts of NADPH oxidase-derived ROS and recruit-

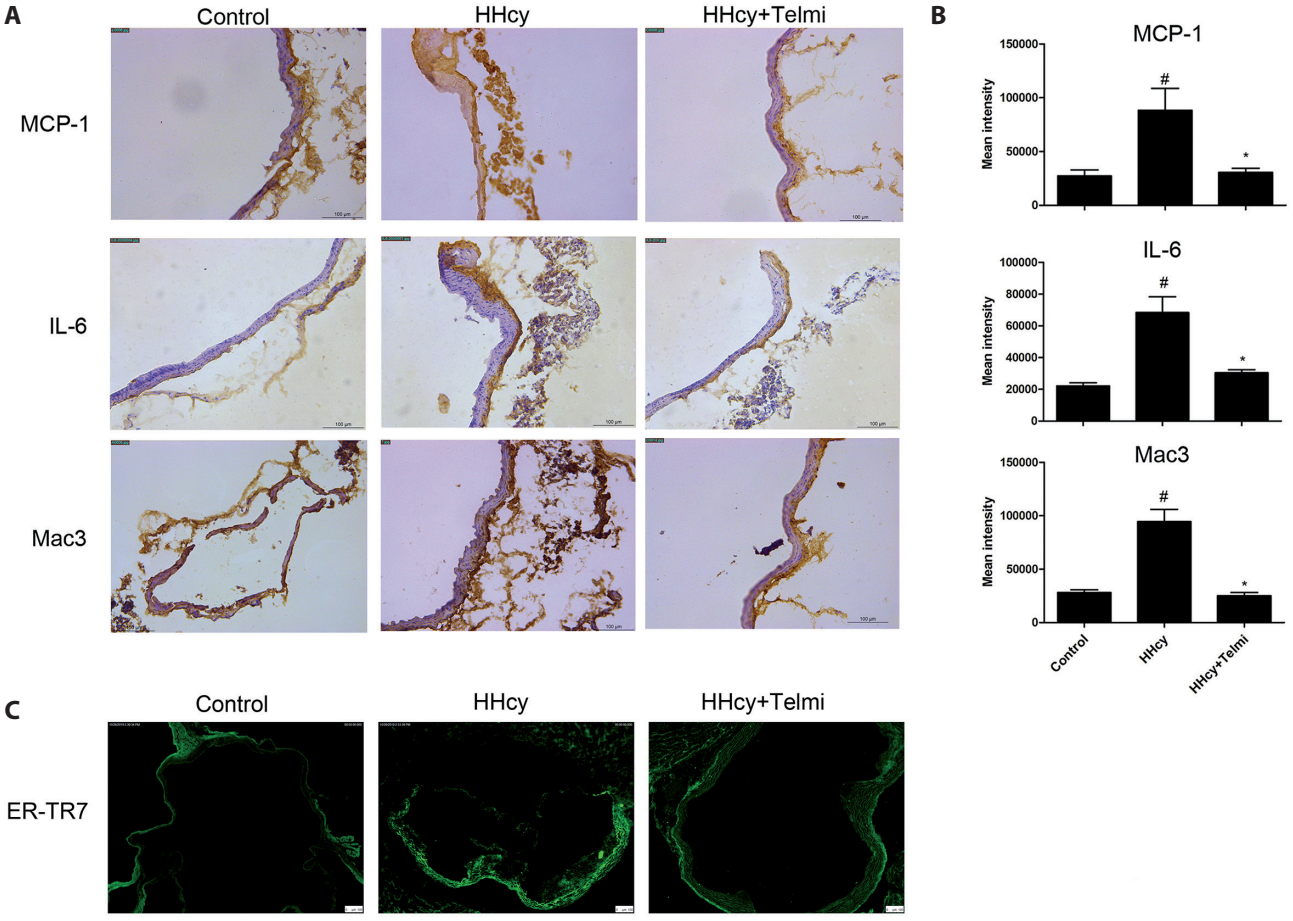

Figure 3. AT1R mediates HHcy-promoted inflammation of aortic adventitia in ApoE$^{-/-}$ male mice and HHcy induces AFs migration and invasion. **A.** Representative immunohistochemistry staining of IL-6, MCP-1, and Mac3 infiltration in aortic adventitia in ApoE$^{-/-}$ male mice. **B.** Quantitative analysis of MCP-1, IL-6, and Mac3 infiltration in aortic adventitia. Magnification: ×200. Scale bar = 100 μm. (n = 3 mice for each group). Data represent mean ± SEM. The data were analyzed by one-way ANOVA. $^{\#}$ p <0.05 *vs.* Control; * p < 0.05 *vs.* HHcy. **C.** Representative immunofluorescence staining. Control: few ER-TR7 in adventitia of aorta root; HHcy: more ER-TR7 in the whole aortic wall and plaque; HHcy+Telmi: ER-TR7 decreased after telmisartan treatment and was mainly expressed in adventitia of aorta. Magnification: ×100. Scale bar = 100 μm. For more abbreviations, see Figure 1.

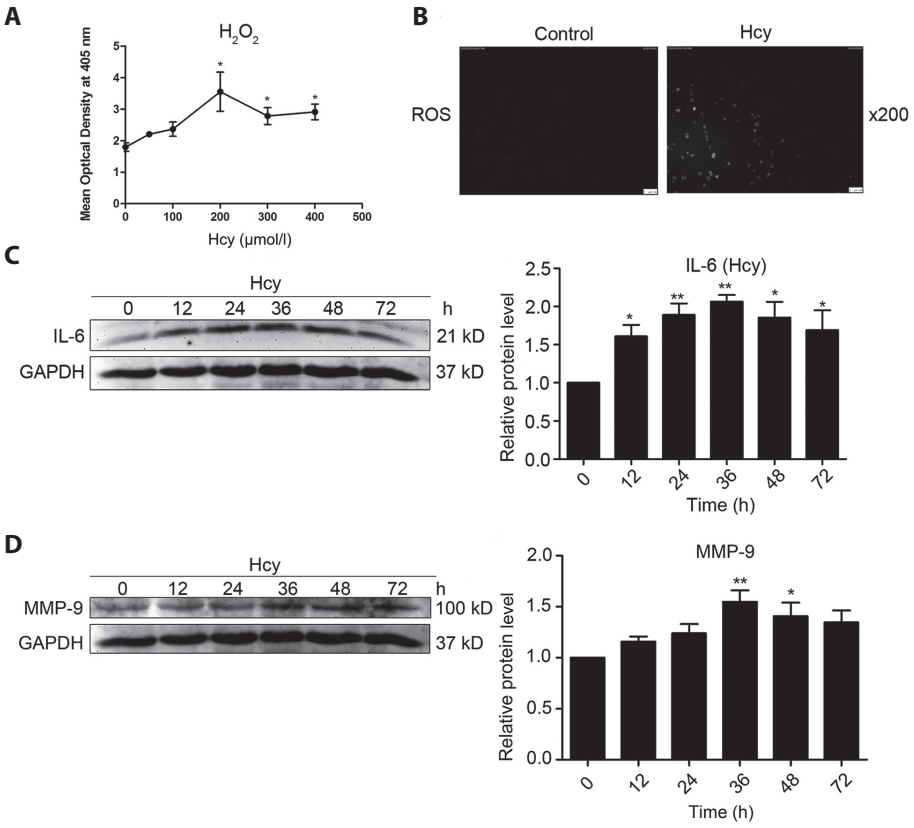

Figure 4. Homocysteine induces inflammation in AFs. **A.** The concentration of H_2O_2 in the cell supernatant was measured by a hydrogen peroxide kit. Homocysteine (Hcy) of 200 μmol/l greatly enhanced H_2O_2 secretion **B.** Fluorescence microscopy showed that the green fluorescence detected by the ROS probe DCFH-DA was brighter in the Hcy group than the Control group, when the cells treated with 200 μmol/l homocysteine were incubated for 48 h. Western blot indicated IL-6 (**C**) and MMP-9 (**D**) levels of cells treated with 200 μmol/l homocysteine in different periods of time (0–72 h) ($n = 3$). Data represents mean ± SEM. The data were analyzed by one-way ANOVA. * $p < 0.05$, ** $p < 0.01$ *vs.* 0 h. Control, untreated cells; Hcy, cells treated with 200 μmol/l homocysteine. (See online version for color figure.)

ing inflammatory cells (Meijles et al. 2016). Homocysteine aggravated aortic adventitial inflammation increased the incidence of AAA in ApoE$^{-/-}$ mice caused by infused angiotensin II. The mechanism of this adverse event was that homocysteine activates NADPH oxidase 4 in adventitial fibroblasts (Liu et al. 2012). Furthermore, HHcy exacerbated vessel remodeling following balloon injury in rats by increasing collagen deposition in adventitia (Guo et al. 2008). However, valsartan, the AT1R antagonist could inhibit this phenomenon, implying the involvement of AT1R in the pathogenic effects of homocysteine on adventitial remodelling (Yao et al. 2014). Genetic deletion of AT1a receptor effectively prevents pathological vascular injuries in a variety of animal models, including models of atherosclerosis and AAA (Tiyerili et al. 2012). Recent data have demonstrated that homocysteine directly interacted and activated with AT1R to aggravate vascular injury in AAA mouse models (Li et al. 2018). However, the underlying mechanisms of HHcy in promoting atherosclerosis remain unknown. Here, we demonstrated that HHcy induced AFs to participate in the formation of atherosclerosis, and the related mechanism may be related to AT1R.

A plethora of evidence details the crucial role that dyslipidemia plays in vascular pathology associated with HHcy. Vascular mitochondrial oxidative stress increases under hyperlipidemic conditions, resulting in enhanced atherosclerotic plaque inflammation, necrotic core and fibrous cap remodeling, and susceptibility to rupture (Vendrov et al. 2017). In this study, ApoE$^{-/-}$ mice receiving methionine diet displayed high levels of serum homocysteine, TC, and typical atherosclerotic plaques, which were accumulated lipid, increased necrotic core, decreased collagen fiber content, and infiltrated inflammation cells in the aortic root. After telmisartan treatment, these effects of HHcy were inhibited. Consistent with the study by Schlimmer, our data revealed that telmisartan can effectively reduce oxidative stress in aortic tissue and subsequent peroxidation of membrane lipids, thereby preventing atherosclerosis formation (Schlimmer et al. 2011; Chan et al. 2016). Based on these results, we speculated that homocysteine might promote atherosclerosis formation *via* AT1R activation. Intriguingly, we found that homocysteine promoted AT1R expression in AFs in a time-and concentration-dependent manner, which was consistent with Dan Yao (Yao et al. 2014). Furthermore, lipid loading increased adventitial metalloproteinase-9 levels to promote cell migration (Kokkinopoulos et al. 2017). We found that HHcy induced AFs migration and invasion *in vitro* and *in vivo*. Telmisartan also inhibited the migration and invasion of fibroblasts induced by HHcy. Homocysteine increased ROS production in AFs,

increased H_2O_2 in cell supernatant, and promoted IL-6 and MMP9 expression in AFs. ROS produced by NADPH oxidase is an important mediator in signal transduction (San et al. 2010). Cell migration in its essence is an invasive process that requires degradation of ECM through activation of matrix metalloproteinases (MMPs) (San et al. 2010). Compelling evidence suggests that AT1R leads to ROS production (Liu et al. 2012). Moreover, ROS can directly or indirectly activate MMPs, hence inducing cell migration. These results suggest that homocysteine may promote AFs migration and invasion by enhancing AT1R expression and then accelerate atherosclerosis formation. The development of atherosclerosis depends largely on local inflammation. A large number of macrophages in atherosclerotic lesions is an indicator of a more unstable and rupture-prone phenotype (Jaffer et al. 2006; Narula et al. 2008). In fact, these cells are aggregated in plaques and swallow lipids, become foam cells, and release cytokines and growth factors, as well as MMPs and ROS that degrade the structures of plaques to provide conditions for cell migration (Libby et al. 2002). Our study also showed that HHcy induced the infiltration of inflammatory cells in aortic root

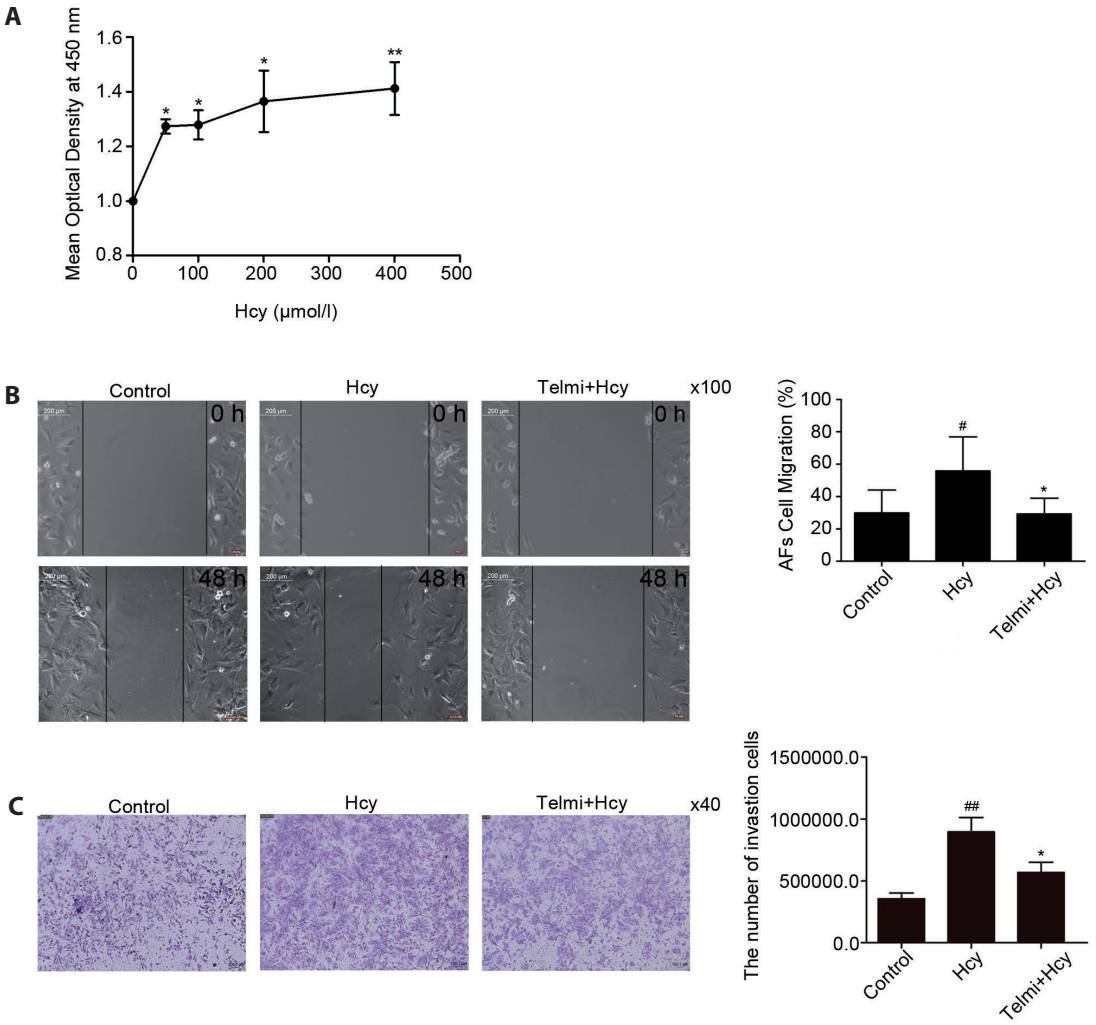

Figure 5. Homocysteine promotes AFs proliferation and induces AFs migration and invasion *via* AT1R. **A.** Cell viability was determined by Cell Counting Kit-8. Cells were treated with homocysteine (0, 50, 100, 200, and 400 μmol/l Hcy) for 48 h, * $p < 0.05$, ** $p < 0.01$ *vs.* 0 μmol/l Hcy. **B.** Cells were scratched and treated with 200 μmol/l homocysteine for 48 h. Image of the wound closure area. Magnification: ×100. Scale bars = 200 μm. $^{\#}$ $p < 0.05$ *vs.* Control; * $p < 0.05$ *vs.* Hcy. **C.** The cells (1×10^5 cells/well) were seeded in invasion chambers after homocysteine treatment for 48 h. Cells were stained with crystal violet. Magnification: ×40. Scale bars = 100 μm. Data represents mean ± SEM ($n = 3$). The data were analyzed by one-way ANOVA if the data that failed to pass the normality test were analyzed by nonparametric test. $^{\#\#}$ $p < 0.01$ *vs.* Control; * $p < 0.05$ *vs.* Hcy. Control, untreated cells; Hcy, cells treated with 200 μmol/l homocysteine; Telmi+Hcy, cells treated with 200 μmol/l homocysteine + telmisartan (10 mmol/l).

plaque and aortic adventitia inflammation in mice, which was consistent with Liu et al. (2012). The results of mice aortic immunohistochemistry showed that infiltrations of MCP-1, IL-6, and Mac3 were mainly observed in the *tunica adventitia* of mice aorta. MCP-1 is a potent chemokine that stimulates cells migration (Wang et al. 2000). There is increasing evidence suggesting that homocysteine has a possible role in triggering arterial inflammation (Lentz et al. 2005; Yun et al. 2011; Liu et al. 2012). ERK1/2 activation has strongly been shown to be associated with inflammation (Morel et al. 2002; Li et al. 2020) and atherosclerosis (Tharaux et al. 2000). A large number of studies have shown

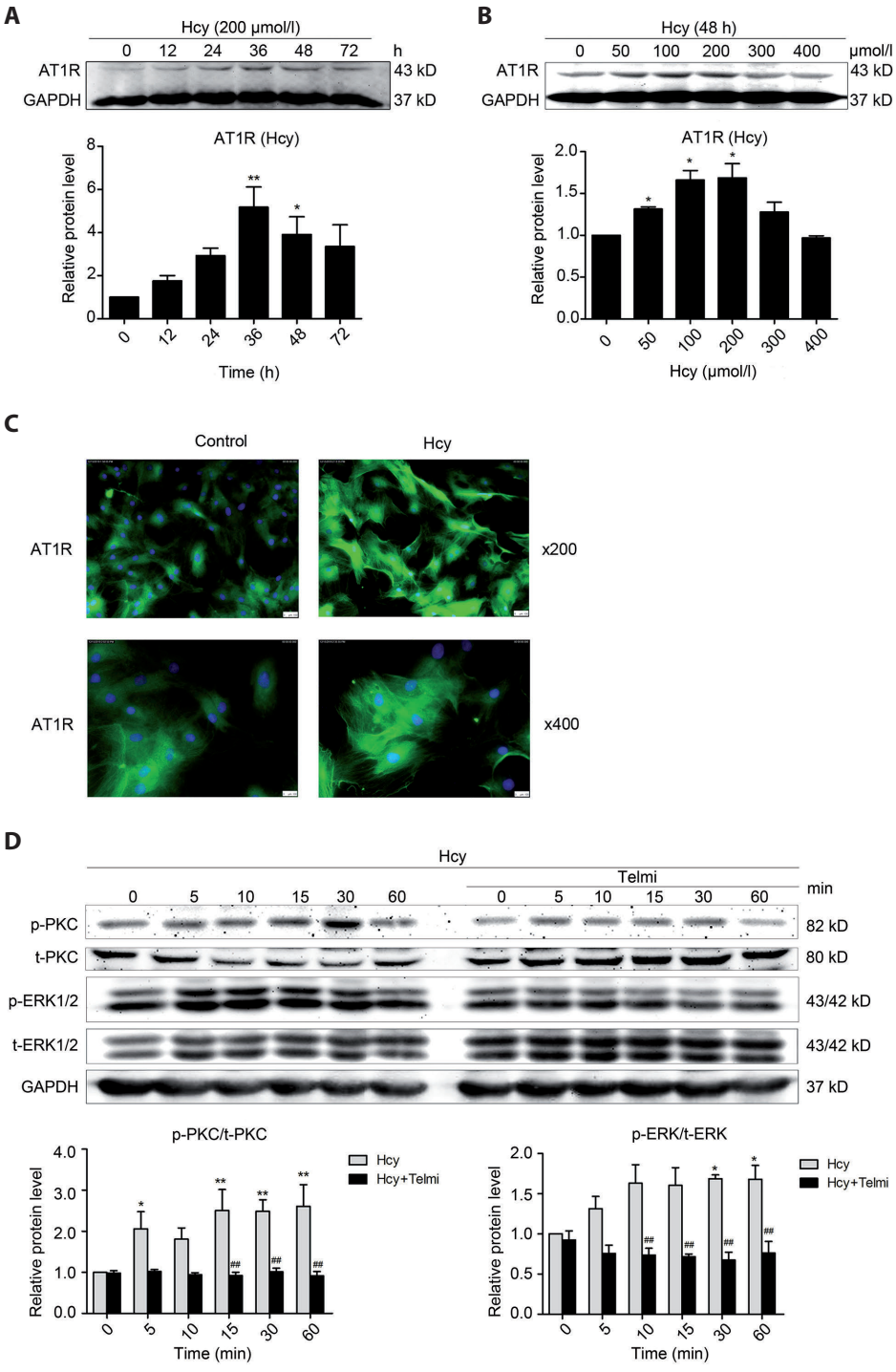

Figure 6. Homocysteine induces AT1R expression and activates the AT1R downstream G protein-dependent signaling pathways in AFs. **A.** Western blot indicated AT1R levels in AFs treated with 200 μmol/l homocysteine (Hcy) in different periods of time (n = 3), * $p < 0.05$, ** $p < 0.01$ *vs.* 0 h. **B.** Western blot indicated that AT1R levels in AFs were treated with various doses of Hcy (0 to 400 μmol/l) for 48 h ($n = 3$), * $p < 0.05$ *vs.* 0 μmol/l Hcy. **C.** Fluorescence microscopy showed that the green fluorescence detected at 48 h-incubation was much brighter in the Hcy group than in the Control group. Magnification: ×200 and ×400. Scale bar = 100 μm. **D.** Representative Western blots and quantification of phosphorylated and total PKC and ERK1/2 in Hcy (200 μmol/l)-treated AFs with or without telmisartan (10 mmol/l) pretreatment for 60 min. Data represents mean ± SEM ($n = 3$). * $p < 0.05$, ** $p < 0.01$ intragroup comparison; # $p < 0.05$, ## $p < 0.01$ between groups. The data were analyzed by repeated measurement ANOVA. (See online version for color figure.)

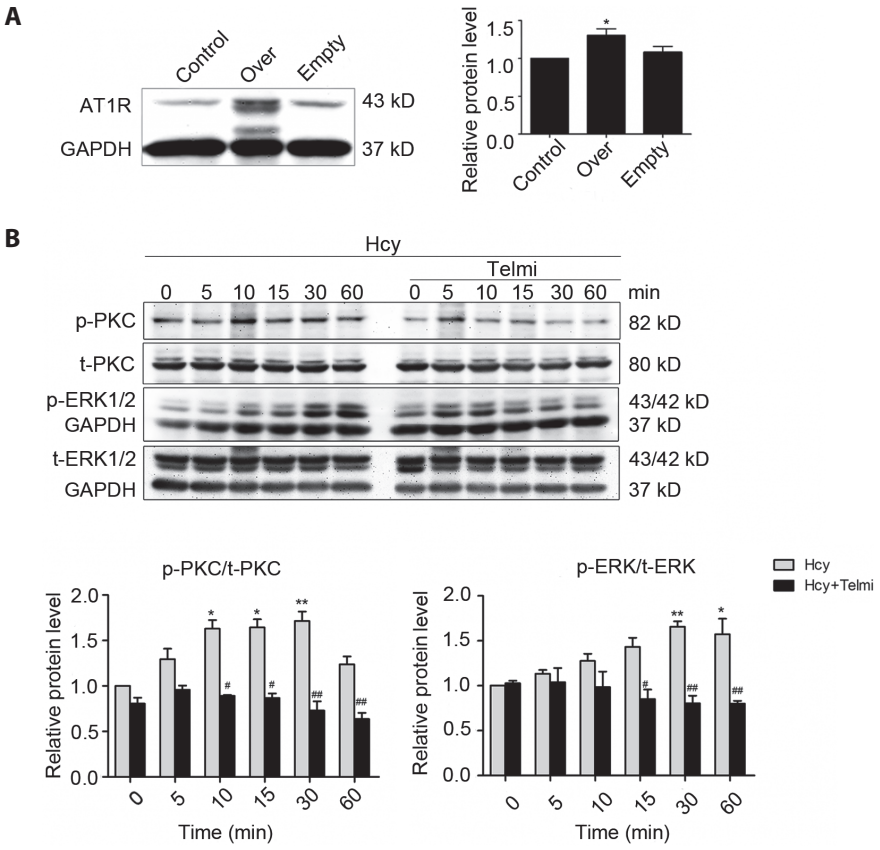

Figure 7. Homocysteine activates the AT1R downstream G protein-dependent signaling pathways in HEK293A cells transfected with human AT1R. **A.** Western blot indicated AT1R levels in HEK293A cells and densitometric analyses (n = 3). Data represents mean ± SEM. The data were analyzed by one-way ANOVA. * $p < 0.05$ *vs.* Control group. Control, HEK293A cells; Over, overexpression of plasmid; Empty, empty plasmid HEK293A cells. **B.** Representative Western blots and quantification of phosphorylated and total PKC and ERK1/2 in homocysteine (Hcy, 200 μmol/l)-treated HEK293A cells (transfected with human AT1R) with or without telmisartan (10 mmol/l) pretreatment for 60 min. Data represents mean ± SEM (n = 3). The data were analyzed by repeated measurement ANOVA. * $p < 0.05$, ** $p < 0.01$ intragroup comparison; $^{\#}p < 0.05$, $^{\#\#}p < 0.01$ between groups.

that ERK and PKC activation can promote cell migration and invasion (Song et al. 2006; Liao et al. 2011). To further explore relevant mechanisms, AFs and HEK293A cells transfected with human AT1R were stimulated by homocysteine, with or without telmisartan pretreatment for 1 hour, and the expression level of ERK1/2 and PKC signaling pathway in AT1R was detected. Our results demonstrated that homocysteine induced a robust and significant increase of ERK1/2 and PKC phosphorylation, which was markedly attenuated by telmisartan. These results clearly suggest the involvement of AT1R in mediating ERK1/2 and PKC phosphorylation in homocysteine.

Of note, we found that telmisartan can reduce homocysteine-induced atherosclerotic plaque *in vivo*. Besides, it was shown that the concentration of homocysteine was significantly decreased in the HHcy+Telmi group compared with that in the HHcy group, and the systolic blood pressure of mice after treatment was lower than that before treatment in HHcy+Telmi group. Therefore, telmisartan might exert protective effects by decreased homocysteine instead of AT1R inhibition or its antihypertensive effect. Intriguingly, we did find that homocysteine could up regulate the expression of AT1R in AFs and induce the migration and invasion of AFs. Telmisartan pretreatment could reduce this phenomenon. Although we did not further knockdown AT1R in AFs and evaluate its migration, previously studies suggested that the atherosclerotic area of $ApoE^{-/-}$/ $AT1a^{-/-}$ mice is smaller than that of $ApoE^{-/-}$ (Eto et al. 2008). Homocysteine at least partially activates AT1R, induces AFs migration and invasion, and aggravates the formation of atherosclerosis.

Conclusion

In conclusion, our experiments confirm that HHcy aggravates atherosclerosis formation, at least in part, by activating AFs through AT1R, causing AFs proliferation, migration, and invasion. These findings suggest that strategies designed to block AT1R may reduce HHcy-related adventitial migration and invasion and thus reduce HHcy-related vascular diseases.

Conflicts of interest. All authors have declared that no competing interests exist.

Ethical approval. Our study was approved by the Institutional Animal Care and Use Committee (No: YKD2015110) of Inner Mongolia Medical University, Hohhot, China.

Funding. The research was supported by funding from the National Natural Science Foundation of the China (81560082).

Acknowledgements. We were grateful for the technical support and kind provision of HEK293A cells by the Inner Mongolia Medical University Laboratory.

References

Chan YK, El-Nezami H, Chen Y, Kinnunen K, Kirjavainen PV (2016): Probiotic mixture VSL#3 reduce high fat diet induced vascular inflammation and atherosclerosis in ApoE(-/-) mice. AMB Express **6,** 61 https://doi.org/10.1186/s13568-016-0229-5

Duan HY, Li YQ, Yan LJ, Yang HT, Wu JT, Qian P, Li B, Wang SL (2016): MicroRNA-217 suppresses homocysteine-induced proliferation and migration of vascular smooth muscle cells via N-methyl-D-aspartic acid receptor inhibition. Clin. Exp. Pharmacol. Physiol. **43,** 967-975 https://doi.org/10.1111/1440-1681.12611

Eto H, Miyata M, Shirasawa T, Akasaki Y, Hamada N, Nagaki A, Orihara K, Biro S, Tei C (2008): The long-term effect of angiotensin II type 1a receptor deficiency on hypercholesterolemia-induced atherosclerosis. Hypertens. Res. **31,** 1631-1642 https://doi.org/10.1291/hypres.31.1631

Fukuda D, Enomoto S, Hirata Y, Nagai R, Sata M (2010): The angiotensin receptor blocker, telmisartan, reduces and stabilizes atherosclerosis in ApoE and AT1aR double deficient mice. Biomed. Pharmacother. **64,** 712-717 https://doi.org/10.1016/j.biopha.2010.09.014

Guo YH, Chen FY, Wang GS, Chen L, Gao W (2008): Diet-induced hyperhomocysteinemia exacerbates vascular reverse remodeling of balloon-injured arteries in rat. Chin. Med. J. **121,** 2265-2271 https://doi.org/10.1097/00029330-200811020-00011

He WM, Dai T, Chen J, Wang JA (2019): Leukocyte cell-derived chemotaxin 2 inhibits development of atherosclerosis in mice. ZR News **40,** 317-323 https://doi.org/10.24272/j.issn.2095-8137.2019.030

Jaffer FA, Libby P, Weissleder R (2006): Molecular and cellular imaging of atherosclerosis: emerging applications. J. Am. Coll. Cardiol. **47,** 1328-1338 https://doi.org/10.1016/j.jacc.2006.01.029

Kassab S, Garadah T, Abu-Hijleh M, Golbahar J, Senok S, Wazir J, Gumaa K (2006): The angiotensin type 1 receptor antagonist valsartan attenuates pathological ventricular hypertrophy induced by hyperhomocysteinemia in rats. J. Renin Angiotensin Aldosterone Syst. **7,** 206-211 https://doi.org/10.3317/jraas.2006.039

Kokkinopoulos I, Wong MM, Potter CMF, Xie Y, Yu BQ, Warren DT, Nowak WN, Bras AL, Ni ZC, Zhou Chao, et al. (2017): Adventitial SCA-1+ progenitor cell gene sequencing reveals the mechanisms of cell migration in response to hyperlipidemia. Stem Cell Rep. **9,** 681-696 https://doi.org/10.1016/j.stemcr.2017.06.011

Lentz SR (2005): Mechanisms of homocysteine-induced atherothrombosis. J. Thromb. Haemost. **3,** 1646-1654 https://doi.org/10.1111/j.1538-7836.2005.01364.x

Liao YH, Hsu SM, Yang HL, Tsai MS, Huang PH (2011): Up-regulated ankyrin repeat-rich membrane spanning protein contributes to tumour progression in cutaneous melanoma. Br. J. Cancer **104,** 982-988 https://doi.org/10.1038/bjc.2011.18

Libby P (2002): Inflammation in atherosclerosis. Nature **420,** 868-874 https://doi.org/10.1038/nature01323

Li T, Yu B, Liu ZX, Li JY, Ma ML, Wang YB, Zhu MJ, Yin HY, Wang XF, Fu Y, et al. (2018): Homocysteine directly interacts and activates the angiotensin II type I receptor to aggravate vascular injury. Nat. Commun. **9,** 11 https://doi.org/10.1038/s41467-017-02401-7

Li XD, Hong MN, Chen J, Lu YY, Ye MQ, Ma Y, Zhu DL, Gao PJ (2020): Adventitial fibroblast-derived vascular endothelial growth factor promotes vasa vasorum-associated neointima formation and macrophage recruitment. Cardiovasc. Res. **116,** 708-720 https://doi.org/10.1093/cvr/cvz159

Liu ZY, Luo HG, Zhang L, Huang YQ, Liu B, Ma KY, Feng J, Xie JS, Zheng JG, Hu J, et al. (2012): Hyperhomocysteinemia exaggerates adventitial inflammation and angiotensin II-induced abdominal aortic aneurysm in mice. Circ. Res. **111,** 1261-1273 https://doi.org/10.1161/CIRCRESAHA.112.270520

Lu YY, Chen TS, Qu JL, Pan WL, Sun L, Wei XB (2019): Dihydroartemisinin (DHA) induces caspase-3-dependent apoptosis in human lung adenocarcinoma ASTC-a-1 cells. J. Biomed. Sci. **16,** 16 https://doi.org/10.1186/1423-0127-16-16

Meijles DN, Pagano PJ (2016: Nox and Inflammation in the vascular adventitia. Hypertension **67,** 14-19 https://doi.org/10.1161/HYPERTENSIONAHA.115.03622

Morel JC, Park CC, Zhu K, Kumar P, Ruth JH, Koch AE (2002): Signal transduction pathways involved in rheumatoid arthritis synovial fibroblast interleukin-18-induced vascular cell adhesion molecule-1 expression. J. Biol. Chem. **277,** 34679-34691 https://doi.org/10.1074/jbc.M206337200

Narula J, Garg P, Achenbach S, Motoyama S, Virmani R, Strauss HW (2008): Arithmetic of vulnerable plaques for noninvasive imaging. Nat. Clin. Pract. Cardiovasc. Med. **5,** S2-S10 https://doi.org/10.1038/ncpcardio1247

San MA, Griendling KK (2010): Redox control of vascular smooth muscle migration. Antioxid. Redox Signal. **12,** 625-640 https://doi.org/10.1089/ars.2009.2852

Schlimmer N, Kratz M, Böhm M, Baumhäkel M (2011): Telmisartan, ramipril and their combination improve endothelial function in different tissues in a murine model of cholesterol-induced atherosclerosis. Br. J. Pharmacol. **163,** 804-814 https://doi.org/10.1111/j.1476-5381.2011.01267.x

Siow RC, Mallawaarachchi CM, Weissberg PL (2003): Migration of adventitial myofibroblasts following vascular balloon injury: insights from in vivo gene transfer to rat carotid arteries. Cardiovasc. Res. **59,** 212-221 https://doi.org/10.1016/S0008-6363(03)00292-X

Snigireva AV, Vrublevskaya VV, Skarga YY, Morenkov OS (2019): Cell surface heparan sulfate proteoglycans are involved in the extracellular Hsp90-stimulated migration and invasion of cancer cells. Cell Stress Chaperones **24,** 309-322

https://doi.org/10.1007/s12192-018-0955-5
Song H, Moon A (2006): Glial cell-derived neurotrophic factor (GDNF) promotes low-grade Hs683 glioma cell migration through JNK, ERK-1/2 and p38 MAPK signaling pathways. Neurosci. Res. **56,** 29-38
https://doi.org/10.1016/j.neures.2006.04.019
Sun WL, Pang YL, Liu ZY, Sun LL, Liu B, Xu MJ, Dong YQ, Feng J, Jiang CT, Kong W, Wang X (2015): Macrophage inflammasome mediates hyperhomocysteinemia-aggravated abdominal aortic aneurysm. J. Mol. Cell Cardiol. **81,** 96-106
https://doi.org/10.1016/j.yjmcc.2015.02.005
Tharaux PL, Chatziantoniou C, Fakhouri F, Dussaule JC (2000): Angiotensin II activates collagen I gene through a mechanism involving the MAP/ER kinase pathway. Hypertension **36,** 330-336
https://doi.org/10.1161/01.HYP.36.3.330
Tiyerili V, Mueller CFH, Becher UM, Czech T, Eickels MV, Daiber A, Nickenig G, Wassmann S (2012): Stimulation of the AT2 receptor reduced atherogenesis in ApoE(-/-)/AT1A(-/-) double knock out mice. J. Mol. Cell Cardiol. **52,** 630-637
https://doi.org/10.1016/j.yjmcc.2011.12.007
Vendrov AE, Stevenson MD, Alahari S, Pan H, Wickline SA, Madamanchi NR, Runge MS (2017): Attenuated superoxide dismutase 2 activity induces atherosclerotic plaque instability during aging in hyperlipidemic mice. J. Am. Heart Assoc. **6,** e006775
https://doi.org/10.1161/JAHA.117.006775
Venegas-Pino DE, Banko N, Khan MI, Shi Y, Werstuck GH (2013): Quantitative analysis and characterization of atherosclerotic lesions in the murine aortic sinus. J. Vis. Exp. **7,** 50933
https://doi.org/10.3791/50933
Wang G, Siow YL, OK (2000): Homocysteine stimulates nuclear factor kappaB activity and monocyte chemoattractant protein-1 expression in vascular smooth-muscle cells: a possible role for protein kinase C. Biochem. J. **352,** 817-826
https://doi.org/10.1042/bj3520817
Wang J, Liu GM, Li QS, Wang F, Xie F, Zhai RP, Guo YY, Chen TX, Zhang NN, Ni WH, et al. (2015): Mucin1 promotes the migration and invasion of hepatocellular carcinoma cells via JNK-mediated phosphorylation of Smad2 at the C-terminal and linker regions. Oncotarget **6,** 19264-19278
https://doi.org/10.18632/oncotarget.4267
Xu F, Liu Y, Shi L, Liu W, Zhang L, Cai HJ, Qi J, Cui Y, Wang WC, Hu YJ (2015): NADPH oxidase p47phox siRNA attenuates adventitial fibroblasts proliferation and migration in apoE (-/-) mouse. J. Transl. Med. **13,** 38
https://doi.org/10.1186/s12967-015-0407-2
Xu JY, Chang NB, Li T, Jiang R, Sun XL, He YZ , Jiang J (2017): Endothelial cells inhibit the angiotensin II induced phenotypic modulation of rat vascular adventitial fibroblasts. J. Cell Biochem. **118,** 1921-1927
https://doi.org/10.1002/jcb.25941
Xu L, Hao HY , Hao YJ, Wei G, Li GZ, Ma PJ, Xu LB, Ding N, Ma SC, Chen AF, Jiang YD (2019): Aberrant MFN2 transcription facilitates homocysteine-induced VSMCs proliferation via the increased binding of c-Myc to DNMT1 in atherosclerosis. J. Cell. Mol. Med. **23,** 4611-4626
https://doi.org/10.1111/jcmm.14341
Yang AN, Zhang HP, Sun Y, Yang XL, Wang N, Zhu GR, Zhang H, Xu H, Ma SC , Zhang Y, et al. (2015): High-methionine diets accelerate atherosclerosis by HHcy-mediated FABP4 gene demethylation pathway via DNMT1 in ApoE(-/-) mice. FEBS Lett. **589,** 3998-4009
https://doi.org/10.1016/j.febslet.2015.11.010
Yang XL, Zhao L, Li SQ, Ma SC, Yang AN, Ding N, Li N, Jia YX, Yang XM, Li GZ, Jiang YD (2020): Hyperhomocysteinemia in ApoE-/- mice leads to overexpression of enhancer of zeste homolog 2 via miR-92a regulation. PLoS One **15,** e0167744
https://doi.org/10.1371/journal.pone.0240762
Yao D, Sun NL (2014): Hyperhomocysteinemia accelerates collagen accumulation in the adventitia of balloon-injured rat carotid arteries via angiotensin II type 1 receptor. Int. J. Mol. Sci. **15,** 19487-19498
https://doi.org/10.3390/ijms151119487
Yun J, Kim JY, Kim OY, Jang Y, Chae JS, Kwak JH, Lim HH, Park HY, Lee SH, Lee JH (2011): Associations of plasma homocysteine level with brachial-ankle pulse wave velocity, LDL atherogenicity, and inflammation profile in healthy men. Nutr. Metab. Cardiovasc. Dis. **21,** 136-143
https://doi.org/10.1016/j.numecd.2009.08.003
Zhang DH, Chen YQ, Xie XN, Liu JL, Wang QJ, Kong W, Zhu Y (2012): Homocysteine activates vascular smooth muscle cells by DNA demethylation of platelet-derived growth factor in endothelial cells. J. Mol. Cell. Cardiol. **53,** 487-496
https://doi.org/10.1016/j.yjmcc.2012.07.010
Zhang YG, Li J, Li YG, Wei RH (2008): Urotensin II induces phenotypic differentiation, migration, and collagen synthesis of adventitial fibroblasts from rat aorta. J. Hypertens. **26,** 1119-1126
https://doi.org/10.1097/HJH.0b013e3282fa1412
Zhao MX, Wen JL, Wang L, Wang XP, Chen TS (2019): Intracellular catalase activity instead of glutathione level dominates the resistance of cells to reactive oxygen species. Cell Stress Chaperones **24,** 609-619
https://doi.org/10.1007/s12192-019-00993-1
Zhao YS, Shang FQ, Shi WL, Zhang J, Zhang JJ, Liu XY, Li B, Hu XG, Wang LY (2019): Angiotensin II receptor type 1 antagonists modulate vascular smooth muscle cell proliferation and migration via AMPK/mTOR. Cardiology **143,** 1-10
https://doi.org/10.1159/000500038
Zou T, Yang WH, Hou ZL, Yang JF (2010): Homocysteine enhances cell proliferation in vascular smooth muscle cells: role of p38 MAPK and p47phox. Acta Biochim. Biophys. Sin. **42,**908-915
https://doi.org/10.1093/abbs/gmq102

Received: May 9, 2022
Final version accepted: June 17, 2022